J. Appl. Comput. Mech., 6(1) (2020) 52-62
DOI: 10.22055/JACM.2019.28761.1504

ISSN: 2383-4536
jacm.scu.ac.ir

M&MoCS

Shahid Chamran University of Ahvaz

Journal of Applied and Computational Mechanics

Research Paper

Melting Heat Transfer Analysis on Magnetohydrodynamics Buoyancy Convection in an Enclosure: A Numerical Study

K. Venkatadri[1], S. Abdul Gaffar[2], M. Suryanarayana Reddy[3], V. Ramachandra Prasad[4] B. Md. Hidayathulla Khan[5], O. Anwar Beg[6]

[1] *Department of Mathematics, VEMU Institute of Technology, P. Kothakota, India*

[2] *Department of Information Technology, Mathematics Section, Salalah College of Technology, Salalah, Oman*

[3] *Department of Mathematics, JNTUA College of Engineering, Pulivendula, India*

[4] *Department of Mathematics, School of Advanced Sciences, Vellore Institute of Technology, Vellore, India*

[5] *Department of Mathematics, Sir Vishveshwaraiah Institute of Science and Technology, Madanapalle, India*

[6] *Magnetohydrodynamics, Biological Propulsion and Energy Research, Aeronautical and Mechanical Engineering Division, University of Salford, M5 4WT, UK*

Received March 02 2019; Revised May 15 2019; Accepted for publication June 12 2019.
Corresponding author: K. Venkatadri (venkatadri.venki@gmail.com)

Abstract. The roll of melting heat transfer on magnetohydrodynamic natural convection in a square enclosure with heating of bottom wall is examined numerically in this article. The dimensionless governing partial differential equations are transformed into vorticity and stream function formulation and then solved using the finite difference method (FDM). The effects of thermal Rayleigh number (*Ra*), melting parameter (*M*) and Hartmann number (*Ha*) are graphically illustrated. As melting parameter and Rayleigh number increase, the rate of fluid flow and temperature gradients also increase. And in the presence of magnetic field, the temperature gradient reduces and hence, the conduction mechanism is dominated for larger *Ha*. Greater heat transfer rate is observed in the case of uniform heating compared with non-uniform case. The average Nusselt number reduces with increasing magnetic parameter in the both cases of heating of bottom wall.

Keywords: Natural convection, Square enclosure, Finite difference method, Incompressible flow, Melting heat transfer.

1. Introduction

Natural thermal convection driven is an interesting area of research in recent times owing to its wide range of applications in geophysics [1], inner core [2] and in nonlinear physics [3]. Generally, natural convection occurs in the fluid layer due to the horizontal temperature gradient or vertical temperature gradient when the lower wall is heated and the upper wall is cooled. The second case is termed as the Rayleigh-Benard convection (RBC). The RBC study was proposed around 1900 through Benard's experiment [4]. RBC is used to study the convection flow problems due to its simplicity and well-defined control parameters [5]. The practical applications of RBC flows include mantle convection [6], melting [7], solar energy field [8], solidification [9 – 12] electrochemical systems [13, 14], etc. Yoshida and Hamano [6] introduced the mantle convection. The thermal boundary condition of Rayleigh-Bénard convection includes an isothermal bottom heating the fluid in the presence of an isothermal cold top wall and adiabatic vertical walls.

Magnetohydrodynamic (MHD) convection flows have several applications in the process of crystal growth, material manufacturing technology, solar technologies and so on. Many researchers have examined the MHD convection flows using various numerical methods as well as analytical techniques such as finite difference method [15, 16], finite element method [17, 18] and analytical method [19, 20]. MHD convection in a trapezoidal enclosure with different inclination

Published online: July 06 2019

angle was reported by Rahman *et al*. [21]. Shehadeh and Duwairi [22] reported the role of inclination angle of an enclosure on MHD convective flow in a porous medium. Finite element based numerical analysis of unsteady MHD convection heat and mass transfer in a semi-circular enclosure with different inclination angle and was examined by Rahman *et al*. [23]. The magnetic field effect on natural convective flow in a square cavity with melting behavior was considered by Doostani *et al*. [24]. Entropy generation in MHD double diffusion natural convection using Lattice-Boltzmann technique was presented by Sathiyamoorthi *et al*. [25]. An increase in entropy generation was observed due to the change in Raleigh number and a reverse trend was observed due to the change in Hartmann number.

The convection flow problems within enclosures are classified into two categories: enclosures subjected to differential lateral heating and enclosures heated from bottom and cooled from the top. The role of non-uniform heat zone of the bottom wall on natural convection in the enclosure was reported by Saravanan and Sivaraj [26]. The effect of surface radiation and non-uniformly heated plate on natural convection fluid flow was illustrated by Saravanan and Sivaraj [27]. Borhan *et al*. [28] studied numerically the magnetohydrodynamic double-diffusive mixed convection under the influence of uniform and non-uniform heated bottom wall of the trapezoidal enclosure. Omid [29] examined the combined effect of joule heating and Lorentz forces on MHD natural convection of lid-driven cavity. They investigated the convective flow and heat transfer characteristics within a driven cavity filled with nanofluid under the sinusoidal heated side walls of the enclosure. Sheikholeslami *et al*. [30] conducted the numerical analysis of MHD convection in the cavity in the presence of sinusoidal temperature distribution wall using finite volume element. Cheong *et al*. [31] carried out a numerical study on the influence of sinusoidal thermal boundary condition along an inclined rectangular cavity with various aspect ratios. Salam [32] reported the heatline and entropy analysis on MHD double-diffusive convection in a corrugated porous cavity under the sinusoidal temperature boundary conditions with different inclination angle.

In the past few decades, phase change materials (PCM) have pulled into ever-increasing extent considerations since they have high thermal storage density while requiring less mass and volumes of material [33]. PCMs have wide applications in buildings for space heating / cooling [34], solar energy storage [35] thermal performance improvement of building envelope [36] and many more. For solid-liquid PCM is classified into two categories. If the PCM coverts solid into liquid, it is termed as melting process. While if the liquid turns into solid then it is termed as solidifying process. Xu *et al*. [37] performed LBM simulation of double-diffusive natural convection in a porous enclosure with isothermal cold walls except for inner obstacle while the circular obstacle surface is maintained hot temperature. They inspected the effects of Darcy number, Lewis number and buoyancy ratio on the double-diffusion convection. The PCM melting heat transfer in a cavity under the internal fins using LBM has been proposed by Ren *et al*. [38]. They implemented the GPU accelerated numerical study through lattice Boltzmann method for investigating the conjugate heat transfer. They also investigated the melting process in PCMs for various parametric conditions. And a similar investigation of comparative PCM melting process in a heat pipe carried out by Ren *et al*. [39]. They concluded that the optimum metal foam porosity and heat pipe radius for energy storage efficiency exists. Jiang and Qu [40] reported a comprehensive study on phase change material and heat pipe composite. Zhu *et al*. [41] studied the transient performance of the phase change material base heat sink filled with copper foam experimentally. They observed that the PCM based heat sink inhibits the temperature during the heating process. Ren [42] investigated the melting rate of nanoparticles without affecting the thermal energy storage capacity of the system using LBM.

This article intends to present the influence of melting heat transfer on natural convection of electrically conducting fluid. FDM is selected to find the outputs. The role of Melting parameter, Hartmann and Rayleigh numbers are presented graphically. Additionally, a comparison between the present and existing results is performed to ensure the authentication of the obtained results.

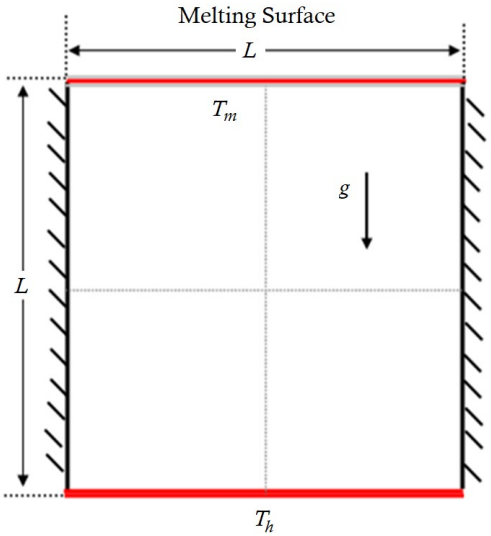

Fig. 1. Physical geometry and the boundary conditions

2. Problem Statement

The physical schematic diagram of the present problem with boundary conditions is depicted in Fig. 1. The bottom wall of the enclosure is uniformly heated and the top surface is considered as the melting surface. And both the vertical walls are thermally insulated. The enclosure is filled with water.

3. Governing Equations

A 2-D unsteady incompressible laminar magnetohydrodynamic convection flow is considered within a square enclosure of length L. The governing partial differential equations are:

$$\frac{\partial u}{\partial x}+\frac{\partial v}{\partial y}=0 \tag{1}$$

$$\rho\left(\frac{\partial u}{\partial t}+u\frac{\partial u}{\partial x}+v\frac{\partial u}{\partial y}\right)=-\frac{\partial p}{\partial x}+\mu\left(\frac{\partial^2 u}{\partial x^2}+\frac{\partial^2 u}{\partial y^2}\right) \tag{2}$$

$$\rho\left(\frac{\partial v}{\partial t}+u\frac{\partial v}{\partial x}+v\frac{\partial v}{\partial y}\right)=-\frac{\partial p}{\partial y}+\mu\left(\frac{\partial^2 v}{\partial x^2}+\frac{\partial^2 v}{\partial y^2}\right)+\rho g\beta\left(T-T_m\right)-\sigma B_0^2 v \tag{3}$$

$$\frac{\partial T}{\partial t}+u\frac{\partial T}{\partial x}+v\frac{\partial T}{\partial y}=\alpha\left(\frac{\partial^2 T}{\partial x^2}+\frac{\partial^2 T}{\partial y^2}\right) \tag{4}$$

$$\begin{gathered}\frac{\partial T}{\partial n}=0 \quad \text{on vertical walls}\\ T=T_h \text{ on bottom wall}\\ T=T_m \quad \text{on top wall}\\ \psi=0 \quad \text{left, right and bottom walls}\end{gathered} \tag{5}$$

and on melting surface, we have

$$k\left(\frac{\partial T}{\partial n}\right)\Big|_{y=1}=\rho\left(L+c_s\left(T_m-T_0\right)\right)\frac{\partial \psi}{\partial n}\Big|_{y=1} \tag{6}$$

To eliminate the pressure source terms, vorticity and stream functions are defined as follows:

$$\omega=\frac{\partial v}{\partial x}-\frac{\partial u}{\partial y}, \quad u=\frac{\partial \psi}{\partial y}, \quad v=-\frac{\partial \psi}{\partial x} \tag{7}$$

The dimensionless quantities are as follows:

$$\tau=\frac{t\alpha}{L^2},(X,Y)=\frac{(x,y)}{L},U=\frac{uL}{\alpha},V=\frac{vL}{\alpha},P=\frac{pL^2}{\rho\alpha^2},\theta=\frac{T-T_m}{T_h-T_m},\Psi=\frac{\psi}{\alpha},\Omega=\frac{\omega L^2}{\alpha} \tag{8}$$

The transformed governing partial differential equations in the form of vorticity – stream function are as follows:

$$\Omega+\frac{\partial^2 \Psi}{\partial X^2}+\frac{\partial^2 \Psi}{\partial Y^2}=0 \tag{9}$$

$$\frac{\partial \Omega}{\partial \tau}+U\frac{\partial \Omega}{\partial X}+V\frac{\partial \Omega}{\partial Y}=\mathrm{Pr}\left(\frac{\partial^2 \Omega}{\partial X^2}+\frac{\partial^2 \Omega}{\partial Y^2}\right)+\mathrm{RaPr}\frac{\partial \theta}{\partial X}-\mathrm{Ha}^2\,\mathrm{Pr}\frac{\partial V}{\partial X} \tag{10}$$

$$\frac{\partial \theta}{\partial \tau}+U\frac{\partial \theta}{\partial X}+V\frac{\partial \theta}{\partial Y}=\frac{\partial^2 \theta}{\partial X^2}+\frac{\partial^2 \theta}{\partial Y^2} \tag{11}$$

The boundary conditions and melting surface condition in the form of vorticity and stream function are adopted from [45].

$$\begin{aligned} \frac{\partial \theta}{\partial n} &= 0 \quad \text{on vertical walls} \\ \theta &= 1 \quad \text{on bottom wall} \\ \theta &= 0 \quad \text{on top wall} \\ \psi &= 0 \quad \text{left, right and bottom walls} \end{aligned} \tag{12}$$

and on melting surface, we have

$$M\theta' + \Pr v = 0 \tag{13}$$

Here

$$Pr = \frac{\upsilon}{\alpha}, \quad Ra = \frac{g\beta \Delta T L^3 Pr}{\upsilon^2}, \quad M = \frac{c_f \left(T_h - T_m\right)}{L + c_s \left(T_m - T_0\right)}, \quad Ha = LB_0 \sqrt{\sigma / \mu} \tag{14}$$

where M is the melting parameter. The Local and average Nusselt numbers over the hot wall are given as follows:

$$\begin{aligned} \frac{\partial \theta}{\partial y} &= Nu \\ Avg.Nu &= \int_0^L Nu\, dx \end{aligned} \tag{15}$$

Table 1. Comparison of Avg. Nu for the present FDM results versus Sathiyamoorthy and Chamkha [43] various *Ha* values.

	Ha	Present work	Ref. [37]
$Gr = 2 \times 10^4$	0	2.5352	2.5439
	10	2.2283	2.2385
	100	1.0062	1.0066
$Gr = 2 \times 10^5$	0	5.0428	5.0245
	10	4.8929	4.9131
	100	1.4267	1.4292

4. Numerical Solution and Validation

The dimensionless governing partial differential equations with relevant thermal, stream function and vorticity boundary conditions are solved using the fine grid finite difference method with the central differences scheme of second order [46]. The diffusive term in the governing equations is approximated using central differences scheme. A second order central difference scheme is applied to the convective term. And Gauss seidal five-point iterative method of central difference scheme is applied to solve the stream function and an explicit time integration is implemented on the momentum and energy equation. The correctness of fine grid finite difference code for natural convection in a trapezoidal cavity is demonstrated in Fig. 2. ([44]) and the natural convective heat transfer of nanofluid in a square enclosure is demonstrated in Fig. 3 ([45]). The validation study is conducted with the MHD natural convection of water within a square enclosure. Table 1 presents the average Nusselt number of the present study compared with the results of Sathiyamoorthy and Chamkha [43] and results are found to be in good agreement. The grid sensitivity test for rigorous grid sizes is presented in Table 2. From Table 2 it can be observed that the average Nusselt number does not yield any substantial change for the grid size above 81 x 81. A mesh size 81 *x* 81 is chosen in the present analysis.

Table 2. Grid sensitivity analysis ($Ra = 10^4$, $Pr = 6.8$, $Ha = 20$)

Grid Size	Avg. Nu
41 x 41	1.0921
51 x 51	1.0888
61 x 61	1.0825
71 x 71	1.0753
81 x 81	1.0673
91 x 91	1.0662
101 x 101	1.0652

5. Results and Discussion

In the present article, the melting heat transfer on magnetohydrodynamic natural convection of water ($Pr = 6.8$) filled in a square enclosure is presented in the presence of uniform and non-uniform heating of bottom wall. The results are computed for various values of melting parameter (M = 0 to 0.8), Hartmann number (Ha = 0 to 30) and Rayleigh number ($Ra = 10^3$ to 10^4).

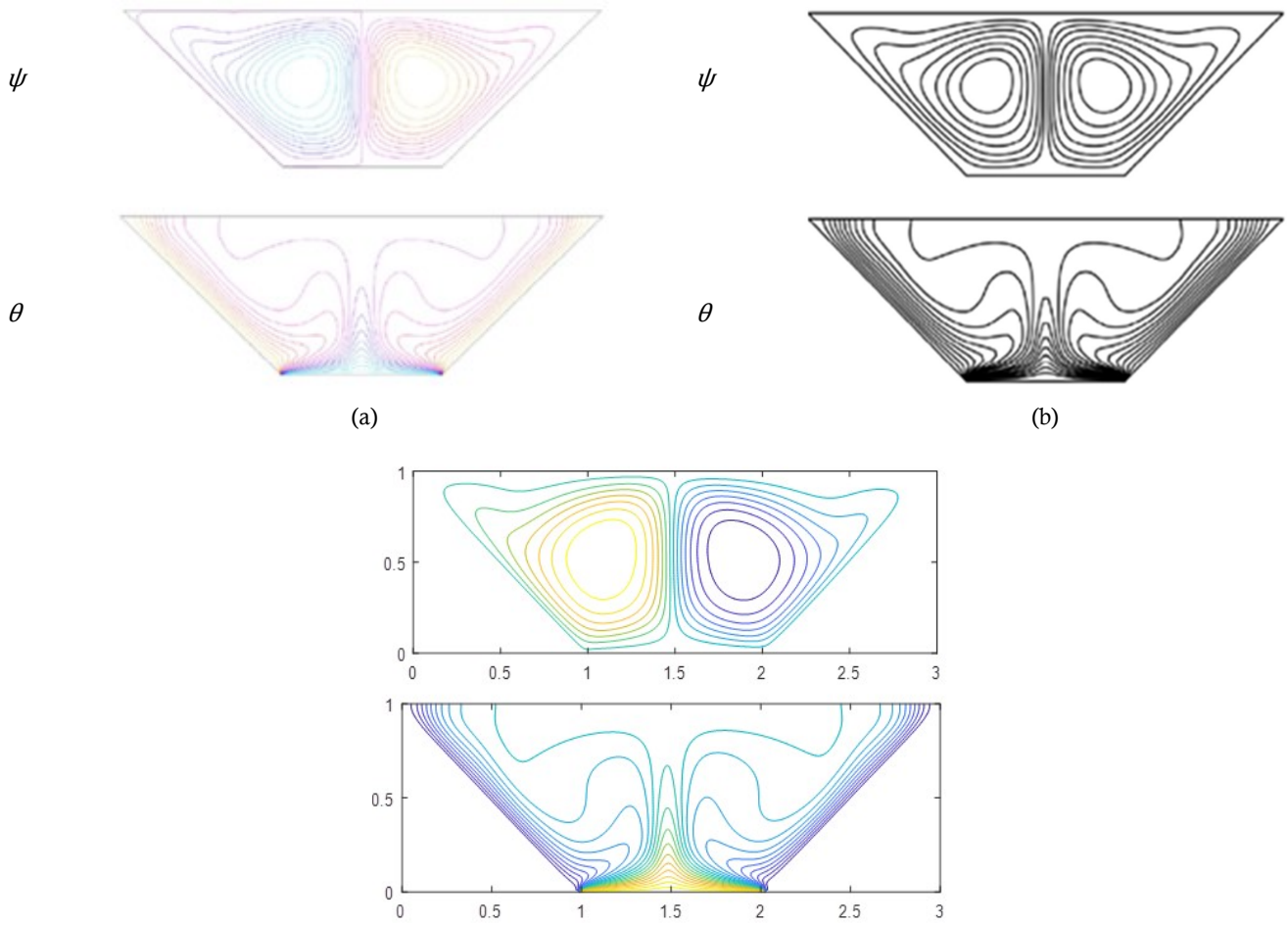

Fig. 2. Comparison results of streamlines and isotherms for $Pr = 0.7$ and $Ra = 10^5$, (a) FLUENT data (b) M.A. Sheremet [45] (c) In-house computational data

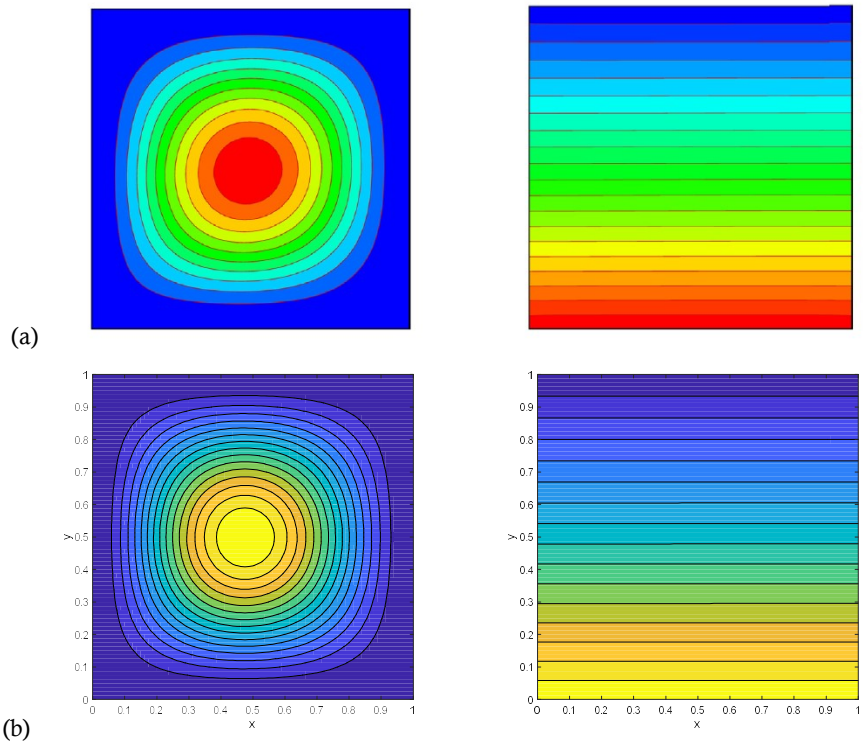

Fig. 3. Comparison of Streamlines and isotherms between (a) Sheikholeslami [45] and (b) In-house computational code of the present study for $Ra = 10^3$, $\phi = 0.04$ and $M = 0$

The effect of Hartmann number, Ha on streamlines with an increase in Ra in the presence of uniform heating is presented in Fig. 4. In the absence of magnetic field the semi-circular stream lines spanned the enclosure starting from top wall. Multiple circulation are formed within the enclosure with an increase in Ha with $Ra = 10^3$ and $Ra = 10^4$.
The temperature contours are depicted in Fig. 5. Regardless of Ha, smooth temperature contours occupied the whole cavity. Moreover, the isotherm lines are parallel to horizontal wall for $Ra = 10^3$, in which case conduction mechanism dominates. As the Ra increases, the distortion of temperature contours enhances close to the hot bottom wall in the absence of magnetic field and the temperature contours get parallel in the presence of magnetic field.
Isotherms and streamlines for different Ra with an increase in Ha are illustrated in Fig. 6 in the presence of sinusoidal temperature distribution at the bottom wall. For $Ra = 10^3$ and in the absence of Ha, the streamlines are in the form of rotating cells as observed in Fig. 6a. However, in the presence of the magnetic field two convective cells are formed as shown in Fig. 6a. For $Ra = 10^4$ and $Ha = 0$, the convective circulation is strengthened more and the enlarged major eddy occupies 98% of the enclosure and a minor eddy is formed at the bottom corner of the left vertical wall as observed in Fig. 6b. In addition, with an increase in Ha, the convective cell circulations become weaker.

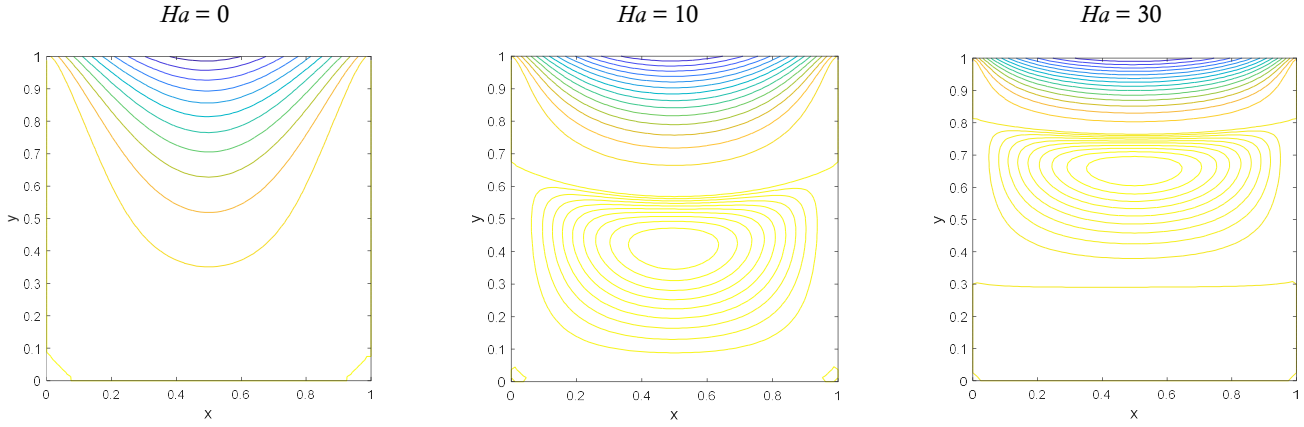

Fig. 4(a) Streamlines for different values of Hartmann numbers for $M = 0.4$, $\theta = 1$ and $Ra = 10^3$

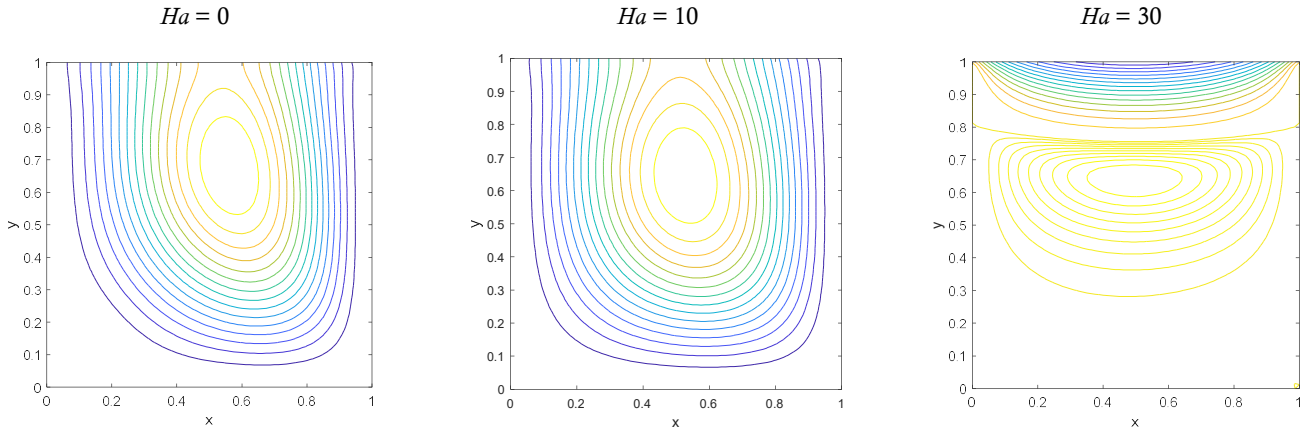

Fig. 4(b) Streamlines for different values Hartmann numbers for $M = 0.4$, $\theta = 1$ and $Ra = 10^4$

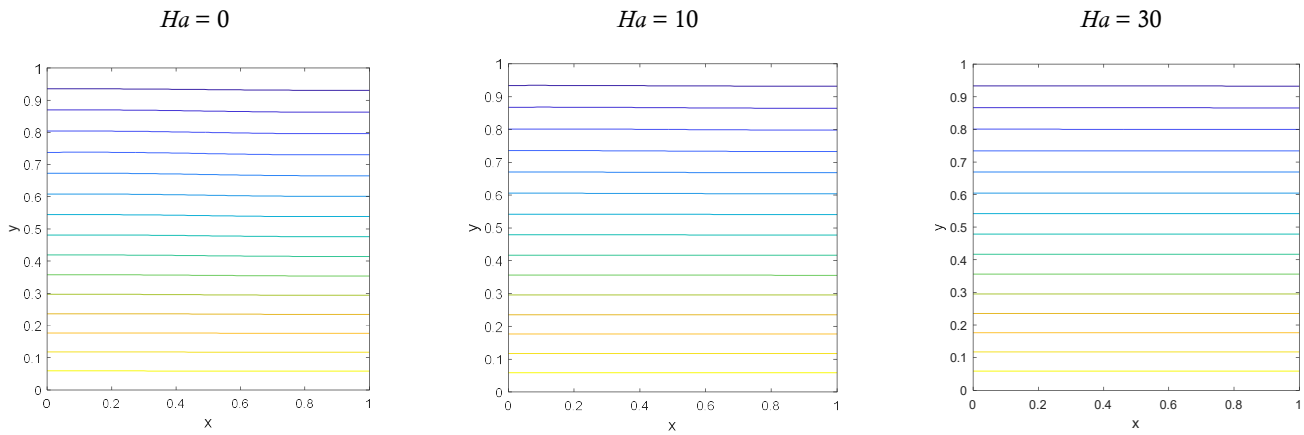

Fig. 5(a) Isotherms for different values Hartmann numbers for $M = 0.4$, $\theta = 1$ and $Ra = 10^3$

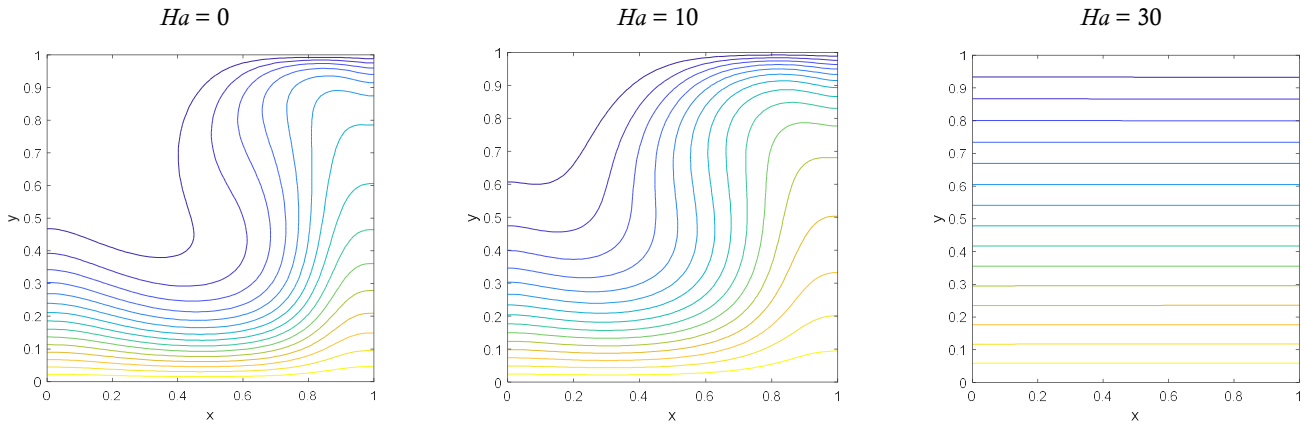

Fig. 5(b) Isotherms for different values Hartmann numbers for $M = 0.4$, $\theta = 1$ and $Ra = 10^4$

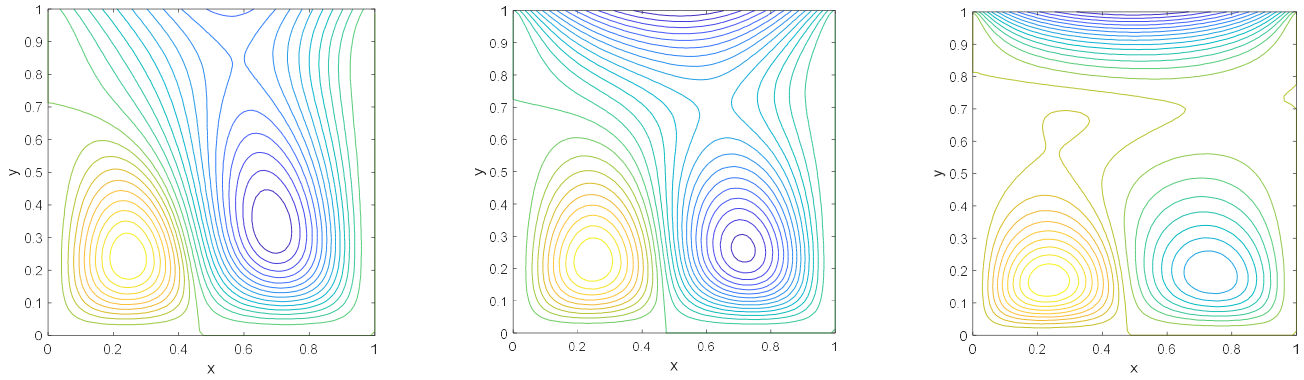

Fig. 6(a) Streamlines for different values Hartmann numbers for $M = 0.4$, $\theta = \sin(\pi X)$ and $Ra = 10^3$

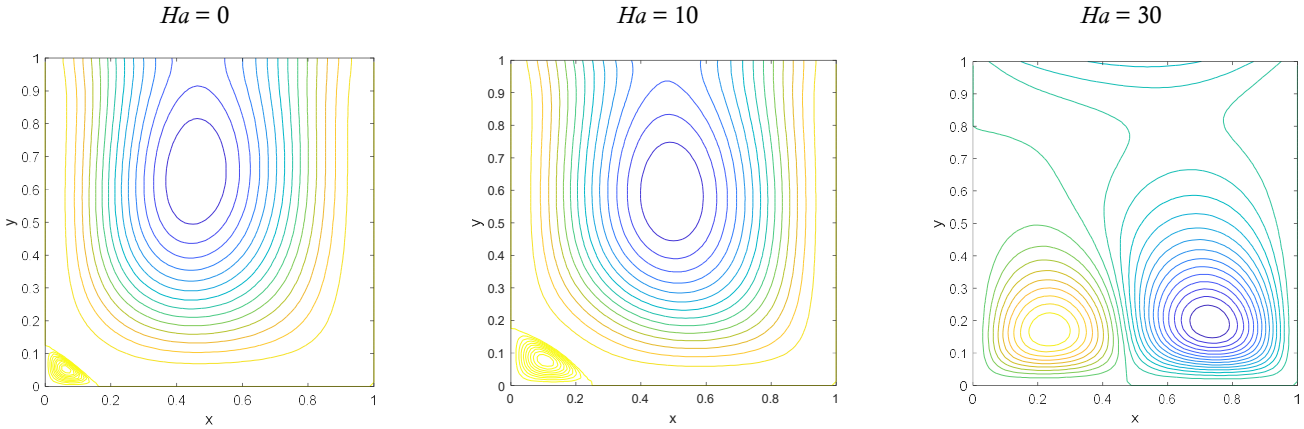

Fig. 6(b) Streamlines for different values Hartmann numbers for $M = 0.4$, $\theta = \sin(\pi X)$ and $Ra = 10^4$

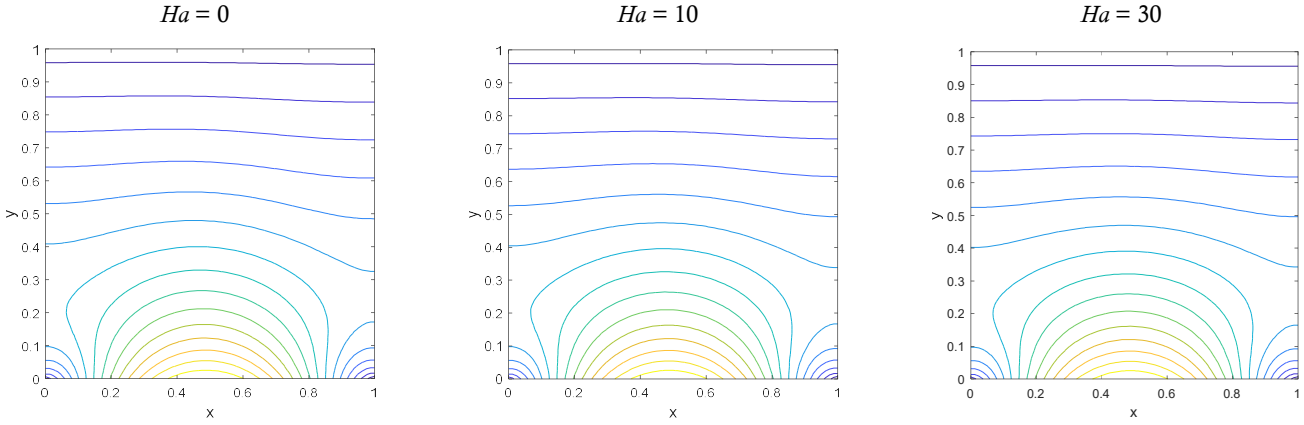

Fig. 7(a) Isotherms for different values Hartmann numbers for $M = 0.4$, $\theta = \sin(\pi X)$ and $Ra = 10^3$

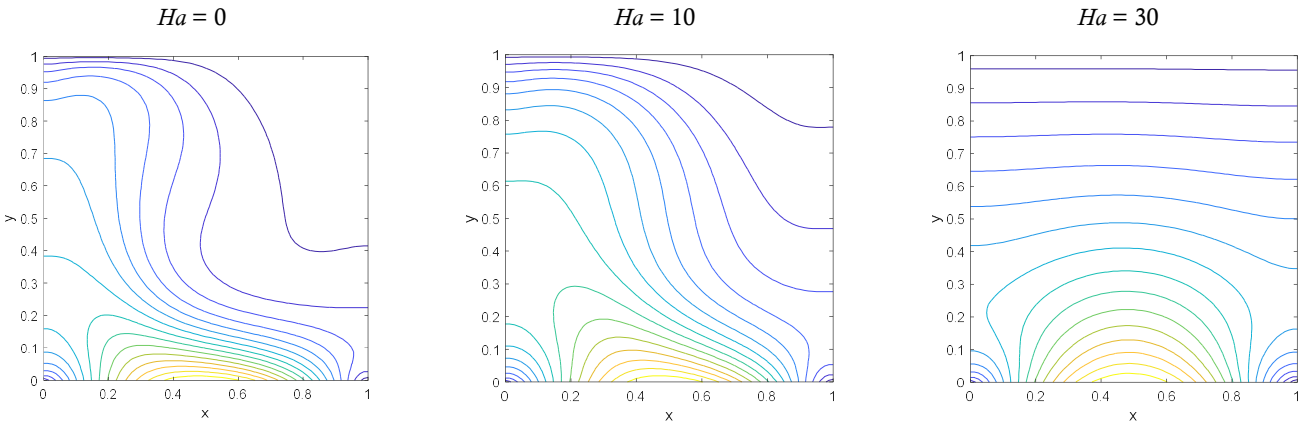

Fig. 7(b) Isotherms for different values Hartmann numbers for $M = 0.4$, $\theta = \sin(\pi X)$ and $Ra = 10^4$

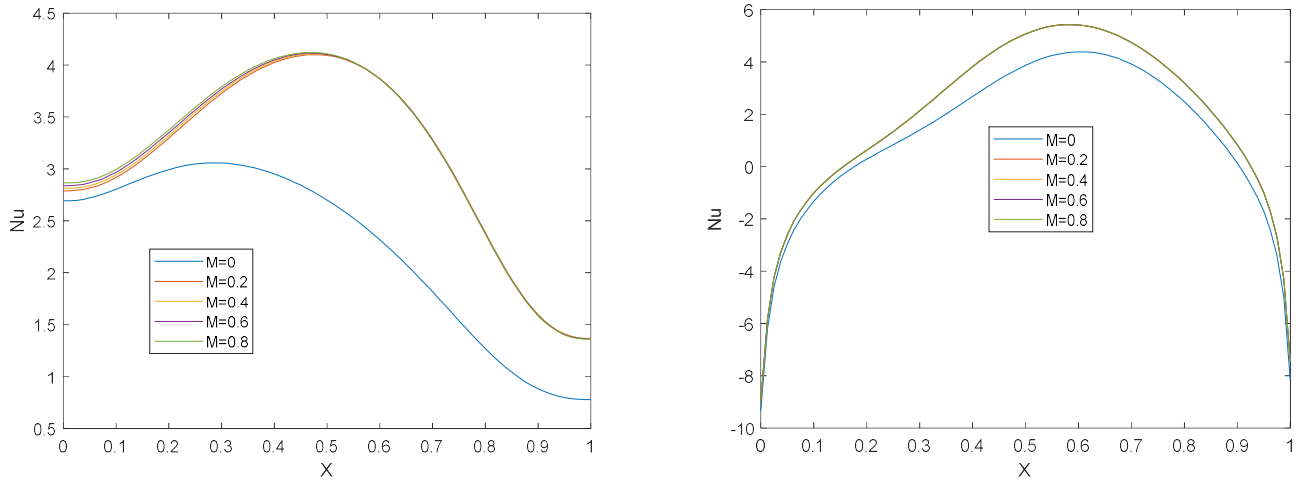

(a) (b)

Fig. 8. Profiles of local Nusselt number of (a) uniform heating of bottom wall and (b) non- uniform heating of bottom wall with melting parameter for $Ra = 10^4$ and $Ha = 0$

However, major changes are observed in the isotherm patterns for increasing values of Ha for $Ra = 10^4$ as shown in Fig. 7b. For large values of Ha, there is a stratification phenomenon in the temperature field appearing at the top half of the cavity and a similar mechanism is observed for $Ra = 10^3$ as well. Profiles of local Nusselt number along the bottom wall for $Ra = 10^4$, $Ha = 0$ and different values of melting parameter in the presence of uniform and non-uniform heating of horizontal bottom wall are presented in Fig. 8. In the absence of melting parameter (i.e., $M = 0$) with the presence of uniform heating of bottom wall, the local Nusselt number is observed to be an increasing function of x-coordinate up to $X = 0.3$ and thereafter a decreasing function is observed.

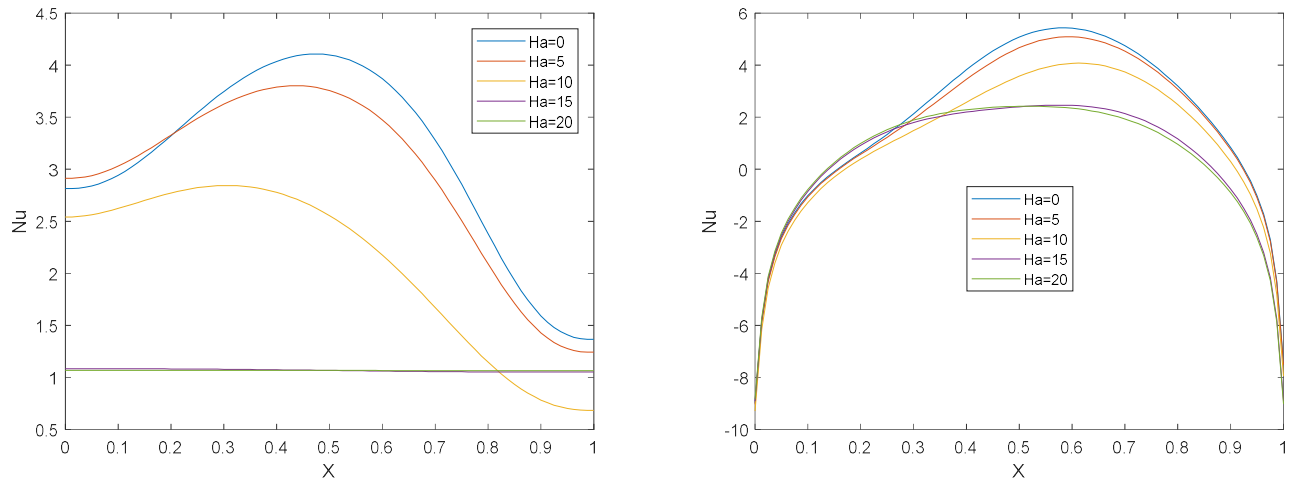

(a) (b)

Fig. 9. Profiles of local Nusselt number of (a) uniformly heated bottom wall and (b) non- uniformly heated bottom wall with Hartmann number $Ra = 10^4$ and $M = 0.4$

However, in the presence of both melting parameter and uniform heating of bottom wall, the heat transfer rate increases along the bottom wall and the maximum heat transfer rate is observed at middle of the bottom wall as shown in Fig. 8(a). The local Nusselt number along the bottom wall for the case of non-uniform heating is shown in Fig. 8(b). The parabolic distribution of the local Nusselt number is observed in the absence and presence of melting parameter. Maximum heat transfer rate is noticed at $X = 0.5$ of the bottom wall and a slight increase in heat transfer rate is seen in the presence of melting parameter (M).

The profiles for local Nusselt number along the bottom wall in the presence of uniform and non-uniform heating for $Ra = 10^4$, $M = 0.4$ for different Ha values are depicted in Fig. 9. A reduction in the local Nusselt number is observed with an increase in Ha values in both the cases of heating of bottom wall. However, for larger values of Ha (i.e., $Ha = 20$), the local Nusselt number is constant along the bottom wall. This is due to fact that the convection dominates the conduction mode. Fig. 10 illustrates the average Nusselt number for uniform and non-uniform heating of bottom wall. A greater heat transfer rate is observed for uniform heating of bottom wall compared to non-uniform heating of bottom wall.

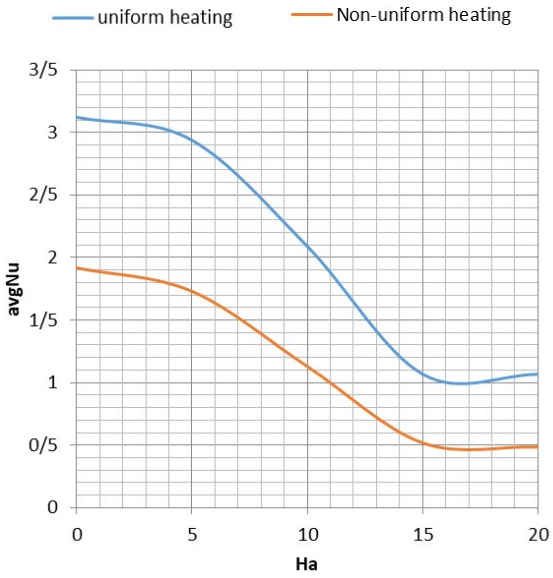

Fig. 10. Variation of average Nusselt number along bottom wall $Ra = 10^4$ and $M = 0.4$

6. Conclusions

In the present study, the fine grid based finite difference technique was used to examine the influence of melting surface on magnetohydrodynamic convection of water filled square cavity. The detailed computational results for the flow patterns, temperature distribution within the cavity and the local and average Nusselt numbers were presented graphically under the influence of both uniform and non-uniform heating of the bottom wall for a wide range of Hartmann number, Rayleigh number and melting parameter. With an increasing melting parameter and Rayleigh number, the rate of fluid flow and temperature gradients were seen to increase. And in the presence of magnetic field, the temperature gradient reduces and hence the conduction mechanism dominated for larger Ha. Greater heat transfer rate was observed in the case of uniform heating compared with non-uniform case.

Conflict of Interest

The authors declared no potential conflicts of interest with respect to the research, authorship and publication of this article.

Funding

The authors received no financial support for the research, authorship and publication of this article.

Nomenclature

B_0	Magnetic field	Nu	Heat transfer coefficient (Local Nusselt number)
c_f	Specific heat coefficient of the fluid	Pr	Prandtl number
c_s	Heat capacity of the solid surface	U, V	Dimensionless velocity components in X and Y direction respectively
Ra	Rayleigh number		**Greek Symbols**
g	Gravitational acceleration	θ	Dimensionless temperature
Ha	Hartmann number	α	Thermal diffusivity
k	Thermal conductivity	β	Coefficient of thermal expansion

L	Length of an enclosure	σ	Electric conductivity of the fluid
M	Melting parameter	μ	Dynamic viscosity
T	Fluid temperature	Ω	Dimensionless vorticity
T_m	Melting surface temperature	ψ	Non-dimensional stream function
T_0	Solid surface temperature	ρ	Fluid density

References

[1] Stevens, B. Atmospheric moist convection. *Annual Review of Earth and Planetary Sciences*, 33(1), 2005, 605–643.

[2] Roberts, P.H., Theory of the geodynamo. In Treatise on Geophysics (Second Edition) (ed. Gerald Schubert), Oxford: Elsevier, 2015.

[3] Cross, M.C., Hohenberg, P.C., Pattern formation outside of equilibrium. *Reviews of Modern Physics*, 65, 1993, 851–1112.

[4] H. Bénard, Les tourbillons cellulaires dans une nappe liquide, *Revue Générale des Sciences Pures et Appliquées*, 11, 1900, 1261–1271.

[5] Bodenschatz, E., Pesch, W., Ahlers, G., Recent developments in Rayleigh-Bénard Convection, *Annual Review of Fluid Mechanics*, 32(1), 2000, 709–778.

[6] Yoshida, M., Hamano, Y., Numerical studies on the dynamics of two-layer Rayleigh-Bénard convection with an infinite Prandtl number and large viscosity contrasts, *Physics of Fluids*, 28, 2016, 116601.

[7] Kumar, S., Roy, S., The effect of Marangoni-Rayleigh-Bénard convection on the process parameters in blown-powder laser cladding process – a numerical investigation, *Numerical Heat Transfer, Part A: Applications*, 50, 2006, 689–704.

[8] Ridouane, E.H., Hasnaoui, M., Campo, A., Effects of surface radiation on natural convection in a Rayleigh-Bénard square enclosure: steady and unsteady conditions, *Heat and Mass Transfer*, 42, 2006, 214–225.

[9] Mackie, C., Desai, P., Meyers, C., Rayleigh-Bénard stability of a solidifying porous medium, *International Journal of Heat and Mass Transfer*, 42, 1999, 3337–3350.

[10] Mackie, C., Convective stability of a particle-laden fluid system in the presence of solidification, *International Journal of Heat and Mass Transfer*, 43, 2000, 1617–1627.

[11] Chakraborty, S., Chakraborty, N., Kumar, P., Dutta, P., Studies on turbulent momentum, heat and species transport during binary alloy solidification in a top-cooled rectangular cavity, *International Journal of Heat and Mass Transfer*, 46, 2003, 1115–1137.

[12] Vikas, D., Basu, S., Dutta, P., In-situ measurements of concentration and temperature during transient solidification of aqueous solution of ammonium chloride using laser interferometry, *International Journal of Heat and Mass Transfer*, 55, 2012, 2022–2034.

[13] Bograchev, D.A., Davydov, A.D., Volgin, V.M., Linear stability of Rayleigh-Bénard Poiseuille convection for electrochemical system, *International Journal of Heat and Mass Transfer*, 51, 2008, 4886–4891.

[14] Amaya-Ventura, G.A., Rodriguez-Romo, S., LBM for cyclic voltammetry of electrochemically mediated enzyme reactions and Rayleigh-Bénard convection in electrochemical reactors, *Heat and Mass Transfer*, 48, 2012, 373– 390.

[15] Sheremet, M.A., Astanina, M.S., Pop, I., MHD natural convection in a square porous cavity filled with a water-based magnetic fluid in the presence of geothermal viscosity, *International Journal of Numerical Methods for Heat & Fluid Flow*, 28(9), 2018, 2111-2131.

[16] Gibanov, N.S., Sheremet, M.A., Oztop, H.F., Al-Salem, K., MHD natural convection and entropy generation in an open cavity having different horizontal porous blocks saturated with a ferrofluid, *Journal of Magnetism and Magnetic Materials*, 452, 2018, 193–204.

[17] Das, D., Lukose, L., Basak, T., Role of multiple discrete heaters to minimize entropy generation during natural convection in fluid filled square and triangular enclosures, *International Journal of Heat and Mass Transfer*, 127, 2018, 1290–1312.

[18] Das, D., Basak, T., Role of discrete heating on the efficient thermal management within porous square and triangular enclosures via heatline approach, *International Journal of Heat and Mass Transfer*, 112, 2017, 489–508.

[19] Alchaar, S., Vasseur, P., Bilgen, E., Hydromagnetic natural convection in a tilted rectangular porous enclosure, *Numerical Heat Transfer, Part A: Applications*, 27, 1995, 107–127.

[20] Aldoss, T.K., Ali, Y.D., Al-Nimr, M.A., MHD mixed convection from a horizontal circular cylinder, *Numerical Heat Transfer, Part A: Applications*, 30, 1996, 379–396.

[21] Hasanuzzaman, M., Öztop, H.F., Rahman, M.M., Rahim, N.A., Saidur, R., Varol, Y., Magnetohydrodynamic natural convection in trapezoidal cavities, *International Communications in Heat and Mass Transfer*, 39, 2012, 1384–1394.

[22] Shehadeh, F.G., Duwairi, H.M., MHD natural convection in porous media-filled enclosures, *Applied Mathematics and Mechanics -Engl. Ed.*, 30(9), 2009, 1113–1120.

[23] Rahman, M.M., Öztop, H.F., Saidur, R., Naim, A.G., Al-Salem, K.S., Ibrahim, T.A., Magnetohydrodynamic time-dependent computational natural convection flow, heat and mass transfer in inclined semi-circular enclosures, *International Journal of Numerical Methods for Heat & Fluid Flow*, 26(8), 2016, 2310-2330.

[24] Doostani, A., Ghalambaz, M., Chamkha, A.J, MHD natural convection phase-change heat transfer in a cavity: analysis of the magnetic field effect, *Journal of the Brazilian Society of Mechanical Sciences and Engineering*, 39(7), 2017, 2831–2846.

[25] Arun, S., Satheesh, A., Mesoscopic analysis of MHD double diffusive natural convection and entropy generation in an enclosure filled with liquid metal, *Journal of the Taiwan Institute of Chemical Engineers*, 95, 2019, 155-173.
[26] Saravanan, S., Sivaraj, C., Natural convection in an enclosure with a localized nonuniform heat source on the bottom wall, *International Journal of Heat and Mass Transfer*, 54, 2011, 2820–2828.
[27] Saravanan, S., Sivaraj, C., Combined natural convection and thermal radiation in a square cavity with a nonuniformly heated plate, *Computers & Fluids*, 117, 2015, 125–138.
[28] Uddin, M.B., Rahman, M.M., Khan, M.A.H., Saidur, R., Ibrahim, T.A., Hydromagnetic double-diffusive mixed convection in trapezoidal enclosure due to uniform and nonuniform heating at the bottom side: Effect of Lewis number, *Alexandria Engineering Journal*, 55, 2016, 1165–1176.
[29] Ghaffarpasand, O., Numerical study of MHD natural convection inside a sinusoidally heated lid-driven cavity filled with $Fe_3 O_4$ -water nanofluid in the presence of Joule heating, *Applied Mathematical Modelling*, 40, 2016, 9165–9182.
[30] Sheikholeslami, M., Oztop, H.F., MHD free convection of nanofluid in a cavity with sinusoidal walls by using CVFEM, *Chinese Journal of Physics*, 55, 2017, 2291–2304.
[31] Cheong, H.T., Siri, Z., Sivasankaran, S., Effect of aspect ratio on natural convection in an inclined rectangular enclosure with sinusoidal boundary condition, *International Communications in Heat and Mass Transfer*, 45, 2013, 75–85.
[32] Hussain, S.H., Analysis of heatlines and entropy generation during double-diffusive MHD natural convection within a tilted sinusoidal corrugated porous enclosure, *Engineering Science and Technology, an International Journal*, 19, 2016, 926–945.
[33] Agyenim, F., Hewitt, N., Eames, P., Smyth, M., A review of materials, heat transfer and phase change problem formulation for latent heat thermal energy storage systems (LHTESSs), *Renewable & Sustainable Energy Reviews*, 14, 2010, 615–28.
[34] Sharma, R.K., Ganesan, P., Tyagi, V.V., Metselaar, H.S.C., Sandaran, S.C., Developments in organic solid–liquid phase change materials and their applications in thermal energy storage, *Energy Conversion and Management*, 95, 2015, 193–228.
[35] Shalaby, S.M., Bek, M.A., Experimental investigation of a novel indirect solar dryer implementing PCM as energy storage medium, *Energy Conversion and Management*, 83, 2014, 1–8.
[36] Memon, S.A., Phase change materials integrated in building walls: a state of the art review, *Renewable & Sustainable Energy Reviews*, 31, 2014, 870–906.
[37] Xu, H.T., Wang, T.T., Qu, Z.G., Chen, J., Li, B.B., Lattice Boltzmann simulation of the double diffusive natural convection and oscillation characteristics in an enclosure filled with porous medium, *International Communications in Heat and Mass Transfer*, 81, 2017, 104-115.
[38] Ren, Q., Chan, C.L., GPU accelerated numerical study of PCM melting process in an enclosure with internal fins using lattice Boltzmann method, *International Journal of Heat and Mass Transfer*, 100, 2016, 522-535.
[39] Ren, Q., Meng, F., Guo, P., A comparative study of PCM melting process in a heat pipe-assisted LHTES unit enhanced with nanoparticles and metal foams by immersed boundary-lattice Boltzmann method at pore-scale, *International Journal of Heat and Mass Transfer*, 121, 2018, 1214-1228.
[41] Jiang, Z.Y., Qu, Z.G., Lithium–ion battery thermal management using heat pipe and phase change material during discharge–charge cycle: A comprehensive numerical study, *Applied Energy*, 242, 2019, 378-392.
[41] Zhu, Z.Q., Huang, Y.K., Hu, N., et al. Transient performance of a PCM-based heat sink with a partially filled metal foam: Effects of the filling height ratio, *Applied Thermal Engineering*, 128, 2018, 966-972.
[42] Ren, Q., Enhancement of nanoparticle-phase change material melting performance using a sinusoidal heat pipe, *Energy Conversion and Management*, 180, 2019, 784-795.
[43] Sathiyamoorthy, M., Chamkha, A.J., Natural convection flow under magnetic field in a square cavity for uniformly (or) linearly heated adjacent walls, *International Journal of Numerical Methods for Heat & Fluid Flow,* 22, 2012, 677–98.
[44] Gibanov, N.S., Sheremet, M.A., Pop, I., Free convection in a trapezoidal cavity filled with a micropolar fluid, *International Journal of Heat and Mass Transfer*, 99, 2016, 831–838.
[45] Sheikholeslami, M., Rokni, H.B., Melting heat transfer influence on nanofluid flow inside a cavity in existence of magnetic field, *International Journal of Heat and Mass Transfer*, 114, 2017, 517–526.
[46] Erturk, E., Gokcol, C., Fourth-order compact formulation of Navier–Stokes equations and driven cavity flow at high Reynolds numbers, *International Journal for Numerical Methods in Fluids*, 50, 2006, 421–436.